Measurements of Higher-Order Flow Harmonics in Au+Au Collisions at $\sqrt{s_{NN}} = 200$ GeV

A. Adare,[11] S. Afanasiev,[27] C. Aidala,[40] N.N. Ajitanand,[57] Y. Akiba,[51,52] H. Al-Bataineh,[46] J. Alexander,[57] K. Aoki,[33,51] Y. Aramaki,[10] E.T. Atomssa,[34] R. Averbeck,[58] T.C. Awes,[47] B. Azmoun,[5] V. Babintsev,[22] M. Bai,[4] G. Baksay,[18] L. Baksay,[18] K.N. Barish,[6] B. Bassalleck,[45] A.T. Basye,[1] S. Bathe,[6] V. Baublis,[50] C. Baumann,[41] A. Bazilevsky,[5] S. Belikov,[5,*] R. Belmont,[62] R. Bennett,[58] A. Berdnikov,[54] Y. Berdnikov,[54] A.A. Bickley,[11] J.S. Bok,[65] K. Boyle,[58] M.L. Brooks,[36] H. Buesching,[5] V. Bumazhnov,[22] G. Bunce,[5,52] S. Butsyk,[36] C.M. Camacho,[36] S. Campbell,[58] C.-H. Chen,[58] C.Y. Chi,[12] M. Chiu,[5] I.J. Choi,[65] R.K. Choudhury,[3] P. Christiansen,[38] T. Chujo,[61] P. Chung,[57] O. Chvala,[6] V. Cianciolo,[47] Z. Citron,[58] B.A. Cole,[12] M. Connors,[58] P. Constantin,[36] M. Csanád,[16] T. Csörgő,[30] T. Dahms,[58] S. Dairaku,[33,51] I. Danchev,[62] K. Das,[19] A. Datta,[40] G. David,[5] A. Denisov,[22] A. Deshpande,[52,58] E.J. Desmond,[5] O. Dietzsch,[55] A. Dion,[58] M. Donadelli,[55] O. Drapier,[34] A. Drees,[58] K.A. Drees,[4] J.M. Durham,[58] A. Durum,[22] D. Dutta,[3] S. Edwards,[19] Y.V. Efremenko,[47] F. Ellinghaus,[11] T. Engelmore,[12] A. Enokizono,[35] H. En'yo,[51,52] S. Esumi,[61] B. Fadem,[42] D.E. Fields,[45] M. Finger,[7] M. Finger, Jr.,[7] F. Fleuret,[34] S.L. Fokin,[32] Z. Fraenkel,[64,*] J.E. Frantz,[58] A. Franz,[5] A.D. Frawley,[19] K. Fujiwara,[51] Y. Fukao,[51] T. Fusayasu,[44] I. Garishvili,[59] A. Glenn,[11] H. Gong,[58] M. Gonin,[34] Y. Goto,[51,52] R. Granier de Cassagnac,[34] N. Grau,[12] S.V. Greene,[62] M. Grosse Perdekamp,[23,52] T. Gunji,[10] H.-Å. Gustafsson,[38,*] J.S. Haggerty,[5] K.I. Hahn,[17] H. Hamagaki,[10] J. Hamblen,[59] R. Han,[49] J. Hanks,[12] E.P. Hartouni,[35] E. Haslum,[38] R. Hayano,[10] X. He,[20] M. Heffner,[35] T.K. Hemmick,[58] T. Hester,[6] J.C. Hill,[26] M. Hohlmann,[18] W. Holzmann,[12] K. Homma,[21] B. Hong,[31] T. Horaguchi,[21] D. Hornback,[59] S. Huang,[62] T. Ichihara,[51,52] R. Ichimiya,[51] J. Ide,[42] Y. Ikeda,[61] K. Imai,[33,51] M. Inaba,[61] D. Isenhower,[1] M. Ishihara,[51] T. Isobe,[10] M. Issah,[62] A. Isupov,[27] D. Ivanischev,[50] B.V. Jacak,[58,†] J. Jia,[5,57] J. Jin,[12] B.M. Johnson,[5] K.S. Joo,[43] D. Jouan,[48] D.S. Jumper,[1] F. Kajihara,[10] S. Kametani,[51] N. Kamihara,[52] J. Kamin,[58] J.H. Kang,[65] J. Kapustinsky,[36] K. Karatsu,[33] D. Kawall,[40,52] M. Kawashima,[53,51] A.V. Kazantsev,[32] T. Kempel,[26] A. Khanzadeev,[50] K.M. Kijima,[21] B.I. Kim,[31] D.H. Kim,[43] D.J. Kim,[28] E. Kim,[56] E.J. Kim,[8] S.H. Kim,[65] Y.J. Kim,[23] E. Kinney,[11] K. Kiriluk,[11] Á. Kiss,[16] E. Kistenev,[5] L. Kochenda,[50] B. Komkov,[50] M. Konno,[61] J. Koster,[23] D. Kotchetkov,[45] A. Kozlov,[64] A. Král,[13] A. Kravitz,[12] G.J. Kunde,[36] K. Kurita,[53,51] M. Kurosawa,[51] Y. Kwon,[65] G.S. Kyle,[46] R. Lacey,[57] Y.S. Lai,[12] J.G. Lajoie,[26] A. Lebedev,[26] D.M. Lee,[36] J. Lee,[17] K. Lee,[56] K.B. Lee,[31] K.S. Lee,[31] M.J. Leitch,[36] M.A.L. Leite,[55] E. Leitner,[62] B. Lenzi,[55] X. Li,[9] P. Liebing,[52] L.A. Linden Levy,[11] T. Liška,[13] A. Litvinenko,[27] H. Liu,[36,46] M.X. Liu,[36] B. Love,[62] R. Luechtenborg,[41] D. Lynch,[5] C.F. Maguire,[62] Y.I. Makdisi,[4] A. Malakhov,[27] M.D. Malik,[45] V.I. Manko,[32] E. Mannel,[12] Y. Mao,[49,51] H. Masui,[61] F. Matathias,[12] M. McCumber,[58] P.L. McGaughey,[36] N. Means,[58] B. Meredith,[23] Y. Miake,[61] A.C. Mignerey,[39] P. Mikeš,[7,25] K. Miki,[61] A. Milov,[5] M. Mishra,[2] J.T. Mitchell,[5] A.K. Mohanty,[3] Y. Morino,[10] A. Morreale,[6] D.P. Morrison,[5] T.V. Moukhanova,[32] J. Murata,[53,51] S. Nagamiya,[29] J.L. Nagle,[11] M. Naglis,[64] M.I. Nagy,[16] I. Nakagawa,[51,52] Y. Nakamiya,[21] T. Nakamura,[21,29] K. Nakano,[51,60] J. Newby,[35] M. Nguyen,[58] R. Nouicer,[5] A.S. Nyanin,[32] E. O'Brien,[5] S.X. Oda,[10] C.A. Ogilvie,[26] M. Oka,[61] K. Okada,[52] Y. Onuki,[51] A. Oskarsson,[38] M. Ouchida,[21] K. Ozawa,[10] R. Pak,[5] V. Pantuev,[24,58] V. Papavassiliou,[46] I.H. Park,[17] J. Park,[56] S.K. Park,[31] W.J. Park,[31] S.F. Pate,[46] H. Pei,[26] J.-C. Peng,[23] H. Pereira,[14] V. Peresedov,[27] D.Yu. Peressounko,[32] C. Pinkenburg,[5] R.P. Pisani,[5] M. Proissl,[58] M.L. Purschke,[5] A.K. Purwar,[36] H. Qu,[20] J. Rak,[28] A. Rakotozafindrabe,[34] I. Ravinovich,[64] K.F. Read,[47,59] K. Reygers,[41] V. Riabov,[50] Y. Riabov,[50] E. Richardson,[39] D. Roach,[62] G. Roche,[37] S.D. Rolnick,[6] M. Rosati,[26] C.A. Rosen,[11] S.S.E. Rosendahl,[38] P. Rosnet,[37] P. Rukoyatkin,[27] P. Ružička,[25] B. Sahlmueller,[41] N. Saito,[29] T. Sakaguchi,[5] K. Sakashita,[51,60] V. Samsonov,[50] S. Sano,[10,63] T. Sato,[61] S. Sawada,[29] K. Sedgwick,[6] J. Seele,[11] R. Seidl,[23] A.Yu. Semenov,[26] R. Seto,[6] D. Sharma,[64] I. Shein,[22] T.-A. Shibata,[51,60] K. Shigaki,[21] M. Shimomura,[61] K. Shoji,[33,51] P. Shukla,[3] A. Sickles,[5] C.L. Silva,[55] D. Silvermyr,[47] C. Silvestre,[14] K.S. Sim,[31] B.K. Singh,[2] C.P. Singh,[2] V. Singh,[2] M. Slunečka,[7] R.A. Soltz,[35] W.E. Sondheim,[36] S.P. Sorensen,[59] I.V. Sourikova,[5] N.A. Sparks,[1] P.W. Stankus,[47] E. Stenlund,[38] S.P. Stoll,[5] T. Sugitate,[21] A. Sukhanov,[5] J. Sziklai,[30] E.M. Takagui,[55] A. Taketani,[51,52] R. Tanabe,[61] Y. Tanaka,[44] K. Tanida,[33,51,52] M.J. Tannenbaum,[5] S. Tarafdar,[2] A. Taranenko,[57] P. Tarján,[15] H. Themann,[58] T.L. Thomas,[45] M. Togawa,[33,51] A. Toia,[58] L. Tomášek,[25] H. Torii,[21] R.S. Towell,[1] I. Tserruya,[64] Y. Tsuchimoto,[21] C. Vale,[5,26] H. Valle,[62] H.W. van Hecke,[36] E. Vazquez-Zambrano,[12] A. Veicht,[23] J. Velkovska,[62] R. Vértesi,[15,30] A.A. Vinogradov,[32] M. Virius,[13] V. Vrba,[25] E. Vznuzdaev,[50] X.R. Wang,[46] D. Watanabe,[21] K. Watanabe,[61] Y. Watanabe,[51,52] F. Wei,[26]

R. Wei,[57] J. Wessels,[41] S.N. White,[5] D. Winter,[12] J.P. Wood,[1] C.L. Woody,[5] R.M. Wright,[1] M. Wysocki,[11] W. Xie,[52] Y.L. Yamaguchi,[10] K. Yamaura,[21] R. Yang,[23] A. Yanovich,[22] J. Ying,[20] S. Yokkaichi,[51,52] Z. You,[49] G.R. Young,[47] I. Younus,[45] I.E. Yushmanov,[32] W.A. Zajc,[12] C. Zhang,[47] S. Zhou,[9] and L. Zolin[27]

(PHENIX Collaboration)

[1]*Abilene Christian University, Abilene, Texas 79699, USA*
[2]*Department of Physics, Banaras Hindu University, Varanasi 221005, India*
[3]*Bhabha Atomic Research Centre, Bombay 400 085, India*
[4]*Collider-Accelerator Department, Brookhaven National Laboratory, Upton, New York 11973-5000, USA*
[5]*Physics Department, Brookhaven National Laboratory, Upton, New York 11973-5000, USA*
[6]*University of California - Riverside, Riverside, California 92521, USA*
[7]*Charles University, Ovocný trh 5, Praha 1, 116 36, Prague, Czech Republic*
[8]*Chonbuk National University, Jeonju, 561-756, Korea*
[9]*China Institute of Atomic Energy (CIAE), Beijing, People's Republic of China*
[10]*Center for Nuclear Study, Graduate School of Science, University of Tokyo, 7-3-1 Hongo, Bunkyo, Tokyo 113-0033, Japan*
[11]*University of Colorado, Boulder, Colorado 80309, USA*
[12]*Columbia University, New York, New York 10027 and Nevis Laboratories, Irvington, New York 10533, USA*
[13]*Czech Technical University, Zikova 4, 166 36 Prague 6, Czech Republic*
[14]*Dapnia, CEA Saclay, F-91191, Gif-sur-Yvette, France*
[15]*Debrecen University, H-4010 Debrecen, Egyetem tér 1, Hungary*
[16]*ELTE, Eötvös Loránd University, H - 1117 Budapest, Pázmány P. s. 1/A, Hungary*
[17]*Ewha Womans University, Seoul 120-750, Korea*
[18]*Florida Institute of Technology, Melbourne, Florida 32901, USA*
[19]*Florida State University, Tallahassee, Florida 32306, USA*
[20]*Georgia State University, Atlanta, Georgia 30303, USA*
[21]*Hiroshima University, Kagamiyama, Higashi-Hiroshima 739-8526, Japan*
[22]*IHEP Protvino, State Research Center of Russian Federation, Institute for High Energy Physics, Protvino, 142281, Russia*
[23]*University of Illinois at Urbana-Champaign, Urbana, Illinois 61801, USA*
[24]*Institute for Nuclear Research of the Russian Academy of Sciences, prospekt 60-letiya Oktyabrya 7a, Moscow 117312, Russia*
[25]*Institute of Physics, Academy of Sciences of the Czech Republic, Na Slovance 2, 182 21 Prague 8, Czech Republic*
[26]*Iowa State University, Ames, Iowa 50011, USA*
[27]*Joint Institute for Nuclear Research, 141980 Dubna, Moscow Region, Russia*
[28]*Helsinki Institute of Physics and University of Jyväskylä, P.O.Box 35, FI-40014 Jyväskylä, Finland*
[29]*KEK, High Energy Accelerator Research Organization, Tsukuba, Ibaraki 305-0801, Japan*
[30]*KFKI Research Institute for Particle and Nuclear Physics of the Hungarian Academy of Sciences (MTA KFKI RMKI), H-1525 Budapest 114, POBox 49, Budapest, Hungary*
[31]*Korea University, Seoul, 136-701, Korea*
[32]*Russian Research Center "Kurchatov Institute", Moscow, 123098 Russia*
[33]*Kyoto University, Kyoto 606-8502, Japan*
[34]*Laboratoire Leprince-Ringuet, Ecole Polytechnique, CNRS-IN2P3, Route de Saclay, F-91128, Palaiseau, France*
[35]*Lawrence Livermore National Laboratory, Livermore, California 94550, USA*
[36]*Los Alamos National Laboratory, Los Alamos, New Mexico 87545, USA*
[37]*LPC, Université Blaise Pascal, CNRS-IN2P3, Clermont-Fd, 63177 Aubiere Cedex, France*
[38]*Department of Physics, Lund University, Box 118, SE-221 00 Lund, Sweden*
[39]*University of Maryland, College Park, Maryland 20742, USA*
[40]*Department of Physics, University of Massachusetts, Amherst, Massachusetts 01003-9337, USA*
[41]*Institut fur Kernphysik, University of Muenster, D-48149 Muenster, Germany*
[42]*Muhlenberg College, Allentown, Pennsylvania 18104-5586, USA*
[43]*Myongji University, Yongin, Kyonggido 449-728, Korea*
[44]*Nagasaki Institute of Applied Science, Nagasaki-shi, Nagasaki 851-0193, Japan*
[45]*University of New Mexico, Albuquerque, New Mexico 87131, USA*
[46]*New Mexico State University, Las Cruces, New Mexico 88003, USA*
[47]*Oak Ridge National Laboratory, Oak Ridge, Tennessee 37831, USA*
[48]*IPN-Orsay, Universite Paris Sud, CNRS-IN2P3, BP1, F-91406, Orsay, France*
[49]*Peking University, Beijing, People's Republic of China*
[50]*PNPI, Petersburg Nuclear Physics Institute, Gatchina, Leningrad region, 188300, Russia*
[51]*RIKEN Nishina Center for Accelerator-Based Science, Wako, Saitama 351-0198, Japan*
[52]*RIKEN BNL Research Center, Brookhaven National Laboratory, Upton, New York 11973-5000, USA*
[53]*Physics Department, Rikkyo University, 3-34-1 Nishi-Ikebukuro, Toshima, Tokyo 171-8501, Japan*
[54]*Saint Petersburg State Polytechnic University, St. Petersburg, 195251 Russia*
[55]*Universidade de São Paulo, Instituto de Física, Caixa Postal 66318, São Paulo CEP05315-970, Brazil*
[56]*Seoul National University, Seoul, Korea*
[57]*Chemistry Department, Stony Brook University, SUNY, Stony Brook, New York 11794-3400, USA*

[58]Department of Physics and Astronomy, Stony Brook University, SUNY, Stony Brook, New York 11794-3400, USA
[59]University of Tennessee, Knoxville, Tennessee 37996, USA
[60]Department of Physics, Tokyo Institute of Technology, Oh-okayama, Meguro, Tokyo 152-8551, Japan
[61]Institute of Physics, University of Tsukuba, Tsukuba, Ibaraki 305, Japan
[62]Vanderbilt University, Nashville, Tennessee 37235, USA
[63]Waseda University, Advanced Research Institute for Science and Engineering, 17 Kikui-cho, Shinjuku-ku, Tokyo 162-0044, Japan
[64]Weizmann Institute, Rehovot 76100, Israel
[65]Yonsei University, IPAP, Seoul 120-749, Korea

(Dated: August 14, 2019)

Flow coefficients v_n for n = 2, 3, 4, characterizing the anisotropic collective flow in Au+Au collisions at $\sqrt{s_{NN}}$ = 200 GeV, are measured relative to event planes Ψ_n, determined at large rapidity. We report v_n as a function of transverse momentum and collision centrality, and study the correlations among the event planes of different order n. The v_n are well described by hydrodynamic models which employ a Glauber Monte Carlo initial state geometry with fluctuations, providing additional constraining power on the interplay between initial conditions and the effects of viscosity as the system evolves. This new constraint improves precision of the extracted viscosity to entropy density ratio η/s.

PACS numbers: 25.75.Dw, 25.75.Ld

The production of particles in heavy ion collisions at the Relativistic Heavy Ion Collider is anisotropic in directions transverse to the beam. For low momentum particles ($p_T \lesssim 3$ GeV/c), this anisotropy is understood to result from hydrodynamically driven flow of the Quark-Gluon Plasma (QGP) [1–5]. The strength of the flow is measured as Fourier coefficients $v_n = \left\langle e^{i\,n(\phi-\Psi_{\rm RP})}\right\rangle, n = 2, 4, ..$ where ϕ is the azimuthal angle of an emitted particle around the z axis defined by the beam, usually at midrapidity; $\Psi_{\rm RP}$ is the azimuth of the reaction plane defined by the beam direction and the impact vector between the colliding nuclei. The brackets denote averaging over particles and events. The reaction plane is not measurable directly a priori, so the Fourier coefficients are determined with respect to the estimated participant event planes [1]. Recent measurements have primarily focused on the even-order anisotropies v_2 and v_4, evaluated with respect to an event plane Ψ_2, determined from the $n = 2$ correlation.

The $v_2(v_4)$ values obtained this way for a broad range of p_T and centrality have been used to extract the specific viscosity η/s (the ratio of viscosity η to entropy density s) of the hot and dense nuclear matter via hydrodynamic model comparisons [6, 7]. These model comparisons, which incorporate the dynamic evolution of an early-stage strongly-coupled QGP, together with a late-stage hadronic gas, give estimates which span the range $4\pi\frac{\eta}{s}{\sim}1--2$. A conjectured lower bound for the specific viscosity is $4\pi\frac{\eta}{s} = 1$ [8] The rather large uncertainties associated with this range of estimates (100%) are currently dominated by the uncertainty on initial state anisotropy estimates [7, 9]. Specifically, the ends of the range are given by two equally successful parameter sets. The lower bound value is obtained with a standard Glauber Monte Carlo model [10, 11] of the initial state which results in smaller initial anisotropy and thus needs less viscosity to reproduce the measured final state particle anisotropy. The higher value $4\pi\frac{\eta}{s} \sim 2$, corresponds to a larger initial anisotropy in the Color Glass Condensate (CGC) inspired Monte-Carlo-Kharzeev-Levin-Nardi (MC-KLN) model [12, 13] of the initial state.

Recently, significant attention has been given to the study of the influence of initial geometry fluctuations of the initial state anisotropy, which are typically quantified by higher-order generalized "eccentricities" ε_n [14, 15] with the goal of understanding how such fluctuations induce anisotropic particle emission, characterized by v_n (for odd and even n)

$$\frac{dN}{d\phi} \propto 1 + \sum_{n=1} 2\, v_n\, \cos(n[\phi - \Psi_n]), \tag{1}$$

where $v_n = \langle \cos(n[\phi - \Psi_n])\rangle, n = 1, 2, 3, ...$ and the Ψ_n are the generalized participant event planes at all orders for each event. These recent developments suggest that measurements of v_n, especially for $n = 3$, can yield important additional constraints that provide a more precise estimate of $\frac{\eta}{s}$, as well as resolve the correct eccentricity model.

Here we present results for differential measurements following Eq. 1, for Au+Au collisions at $\sqrt{s_{NN}}$=200 GeV. We first show how the measured event planes correlate across large rapidity gaps, and then show resulting v_n moments for midrapidity particles relative to those planes. We find that the measured v_n moments, in conjunction with hydrodynamical model calculations [16, 17], indeed provide new constraining power for both the initial state and η/s.

The results are derived from $\sim 3.0 \times 10^9$ Au+Au events obtained with the PHENIX detector [18] during the 2007 running period. Collision centrality (related to impact parameter) and number of participating nucleons ($N_{\rm part}$) determinations were performed with pre-

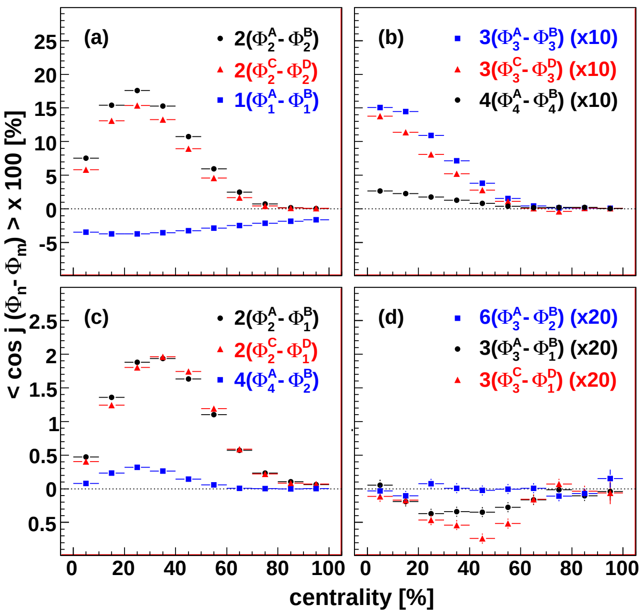

FIG. 1: (color online) Raw correlation strengths (see text) of the event planes for various detector combinations as a function of collision centrality. The detectors in which the event plane is measured are: (a) RXN North, (b) BBC South, (c) MPC North, and (d) MPC South.

viously described methods [19]. Event planes were determined using three separate detector systems: Beam-Beam Counters (BBC) [20], Reaction-Plane Detectors (RXN) [21], and Muon Piston Calorimeters (MPC). Each detector system has a North (South) component to measure at forward (backward) rapidity. The absolute pseudorapidity (η') coverage for these detectors are $3.1 < |\eta'_{\rm BBC}| < 3.9$, $1.0 < |\eta'_{\rm RXN}| < 2.8$, $3.1 < |\eta'_{\rm MPC}| < 3.7$. The PHENIX drift and pad chambers [22] were used for charged particle tracking and momentum reconstruction with azimuthal coverage $\varphi = \pi$ in the central region ($|\eta'| \leq 0.35$).

To estimate the event plane Ψ_n in each detector, we generalize to all orders n our earlier procedure for event plane determination (see [19] and especially definitions in [23]). For each event plane detector we evaluate $\tan(n\Phi_n) = \sum w_i \sin(n\phi_i)/\sum w_i \cos(n\phi_i)$ for the Ψ_n subevent estimator Φ_n, where the ϕ_i are the azimuths of elements in that detector and the weights w_i reflect the energy or multiplicity in that element. Corrections for detector imperfections were also employed to ensure a uniform response. In general, the hit distributions sample virtually all momenta.

To measure v_n, the azimuth ϕ of each particle is correlated with the Ψ_n, and calculated as $v_n\{\Psi_n\} = \langle\cos(n[\phi - \Phi_n^{\rm avg}])\rangle/{\rm Res}(\Psi_n)$ where $\Phi_n^{\rm avg}$ is the average of the Φ_n for North and South subevents and where the denominator ${\rm Res}(\Psi_n)$ represents a resolution factor described in [23]. This factor corrects v_n for the event-by-event dispersion of the Φ_n. Its magnitude can be estimated via the two and three sub-events method [19] in which the correlation between Φ_n from different sub-events is measured. The strength of this correlation is generally quantified as $\left\langle\cos(n[\Phi_n^A - \Phi_n^B])\right\rangle$ for sub-events A, B, which measures the cosine dispersion of Ψ_n.

Figure 1 shows the centrality dependence of this correlation strength $\left\langle\cos(j[\Phi_n^A - \Phi_m^B])\right\rangle$ for sub-event combinations (A, B) involving different event-plane detectors with $\Delta\eta' \sim 5$ and $\Delta\eta' \sim 7$. The raw correlations are presented as measured so that the magnitudes shown should be considered specific to the PHENIX detectors involved. The systematic uncertainties (not shown) for these correlations are of similar relative size to those for $v_n\{\Psi_n\}$ discussed below. The uncertainties are correlated across centrality and n such that the relative size of these event plane correlations can be compared. The magnitudes for the odd parity quantities $\left\langle\sin(j[\Phi_n^A - \Phi_m^B])\right\rangle$, which should vanish, are found to be consistent with zero for all centrality, j, and Φ combinations. Figure 1 panels (a) and (b) show the two sub-events correlations for $m = n$; (c) and (d) show the two sub-events correlations for $m \neq n$. The negative correlation indicated in (a) is due to the well known antisymmetric pseudorapidity dependence of sidewards flow v_1, as well as momentum conservation [2]. Positive sub-event correlations are indicated in (a) and (b) for $\Psi_{2,3,4}$, with sizable magnitudes for $\Psi_{2,3}$ and much smaller values for Ψ_4.

The sub-event correlations $\left\langle\cos(j[\Phi_n^A - \Phi_m^B])\right\rangle$ for $n \neq m$ are also of interest. Fig. 1(c) confirms the expected correlation between Ψ_1 and Ψ_2 (due to sidewards flow), as well as that between Ψ_2 and Ψ_4 [23]. By contrast, Fig. 1(d) shows that there is no significant correlation observed between Ψ_2 and Ψ_3. The order $j = 6$ is chosen to account for the n-multiplet of directions $(2\pi/n)$ of Ψ_2 and Ψ_3. The absence of this correlation suggests that the fluctuations for Ψ_3 about Ψ_2 are substantial. This is well reproduced by Glauber modeling [24, 25] and therefore support an initial state fluctuation origin of Ψ_3 and v_3. A small correlation between Ψ_3 and Ψ_1 is indicated in Fig. 1(d). While such a correlation seems to be at odds with the absence of a $\Psi_2 - \Psi_3$ correlation [cf. Fig. 1(d)], we note that $\Psi_1 - \Psi_3$ correlations need not contribute to a residual contribution to $\Psi_2 - \Psi_3$ correlations through Ψ_1. That is, Ψ_1 could correlate with Ψ_3 and Ψ_2 in exclusive event classes. Comparisons using the PHENIX Zero Degree Calorimeter, which measures the $n = 1$ spectator neutron event plane [23] at $|\eta'| > 6.5$ indicate that this correlation has significant η'-antisymmetry. We defer further investigation of these correlation subtleties to future work.

Fig. 2 shows results for the midrapidity $v_n\{\Psi_n\}$ for tracks in the central arms as a function of p_T for different centralities. They are from the RXN-defined event plane analysis, because this detector has the best resolution. The systematic uncertainties for these measurements were estimated by detailed comparisons of the results obtained with the RXN, BBC, and MPC event plane detectors and subevent selections. They are $\sim 3\%$, $\sim 8\%$ and $\sim 20\%$ for $v_2\{\Psi_2\}$, $v_3\{\Psi_3\}$, and $v_4\{\Psi_4\}$, respectively, for midcentral collisions and increase by a few percent for more central and peripheral collisions. Through further comparison of the results obtained with the RXN, BBC, and MPC event plane detectors, pseudorapidity dependent nonflow contributions that may influence the magnitude of $v_n\{\Psi_n\}$, such as jet correlations, were shown [19] to be much less than all other uncertainties for $v_2\{\Psi_2\}$ and $v_4\{\Psi_2\}$.

The $v_n\{\Psi_n\}$ values shown in Fig. 2 increase with p_T for most of the measured range, and decrease for more central collisions. $v_2\{\Psi_2\}$ and $v_4\{\Psi_4\}$ increase as expected from central to semi-peripheral collisions, which reflects the increase of ε_n in peripheral collisions. $v_3\{\Psi_3\}$ appears to be much less centrality dependent, with values comparable to $v_2\{\Psi_2\}$ in the most central events. This behavior is consistent with Glauber calculations of the average fluctuations of the generalized "triangular" eccentricity ε_3 [24, 25]. The Fig. 2 panels (c), (d), (g), and (h) show comparisons of $v_2\{\Psi_2\}$ and $v_3\{\Psi_3\}$ to results from hydrodynamic calculations. The p_T and centrality trends for both $v_2\{\Psi_2\}$ and $v_3\{\Psi_3\}$ are in good agreement with the hydrodynamic models shown, especially at p_T below ≈ 1 GeV/c.

Figure 3 compares the centrality dependence of $v_2\{\Psi_2\}$ and $v_3\{\Psi_3\}$ with several additional calculations, demonstrating both the new constraints the data provide and also the robustness of hydrodynamics to the details of different model assumptions for medium evolution. Alver et al. [16] use relativistic viscous hydrodynamics in 2+1 dimensions. Fluctuations are introduced for two different initial conditions. For Glauber initial conditions, the energy density distribution in the transverse plane is proportional to a superposition of struck nucleon and binary collision densities; in MC-KLN initial conditions the energy density profile is further controlled by the dependence of the gluon saturation momentum on the transverse position [12, 13]. These two models of the initial state are paired with two different values of $4\pi\frac{\eta}{s} = 1$ and 2, respectively. Both values reproduce the measured $v_2\{\Psi_2\}$ equally well and the viscosity differences reflect the different initial ε_2. The two models have similar ε_3, and thus the larger viscosity needed in the MC-KLN model corresponds to lower v_3 than for Glauber. Consequently, our measurement of $v_3\{\Psi_3\}$ helps to disentangle viscosity and initial conditions. The efficacy of these 2+1 hydrodynamic results for Glauber initial conditions are confirmed further calculations with different model assumptions. Petersen et al. [26] determine a Glauber initial state event-by-event, translating through pre-equilibrium with the UrQMD transport model [27, 28], then evolving the medium with ideal QGP hydrodynamics ($\eta/s = 0$), and finally switching to

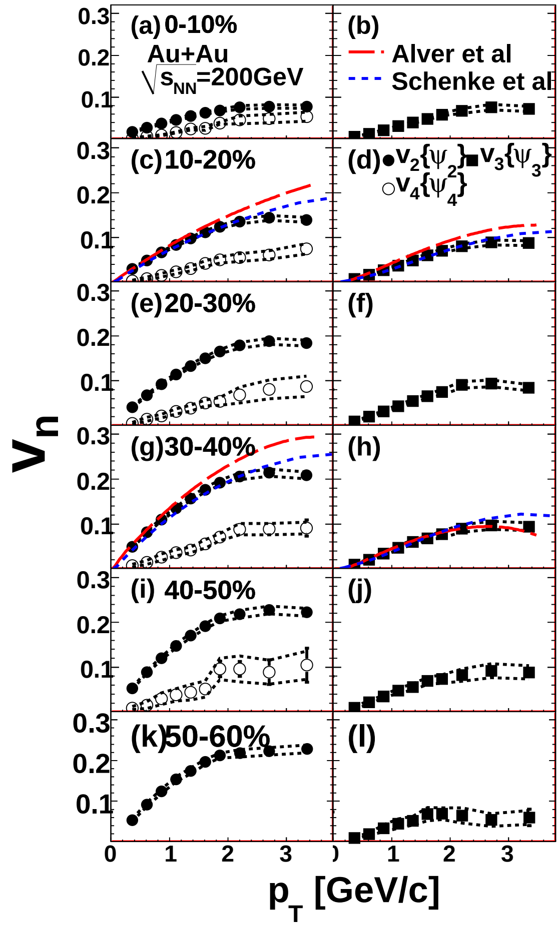

FIG. 2: (color online) $v_n\{\Psi_n\}$ vs. p_T measured via the reaction plane method. The curves are predictions from two hydrodynamic models: Alver *et al.* [16] and Schenke *et al.* [17].

a hadronic cascade (which has an effective viscosity) as regions become dilute. B. Schenke *et al.* [17] use event-by-event Glauber initial conditions, evolved with ideal 3+1 dimensional hydrodynamics, which includes the effects of viscosity in the plasma phase.

All of these models are compared with $v_2\{\Psi_2\}$, and $v_3\{\Psi_3\}$ data as a function of $N_{\rm part}$ in two p_T bins. All calculations describe $v_2\{\Psi_2\}$ well at $p_T = 0.75$ GeV/c. Deviations from hydrodynamics should be expected in peripheral collisions, where nonequilibrium effects may be large. At higher p_T, differences between the calculations become more apparent. All models still agree with $v_2\{\Psi_2\}$, including MC-KLN initial conditions. However, the lower panels of Fig. 3 show the constraining power of $v_3\{\Psi_3\}$ and that the calculated results from viscous hydrodynamics, with MC-KLN initial conditions and $4\pi\frac{\eta}{s} = 2$, lie significantly below the data. This is more apparent in the higher p_T bin, even in the most central collisions. Therefore, our comparisons suggest that the combination of MC-KLN initial conditions in concert with $4\pi\frac{\eta}{s} = 2$ is disfavored by our new $v_3\{\Psi_3\}$ measurements. By contrast, the results from the hydrodynamical

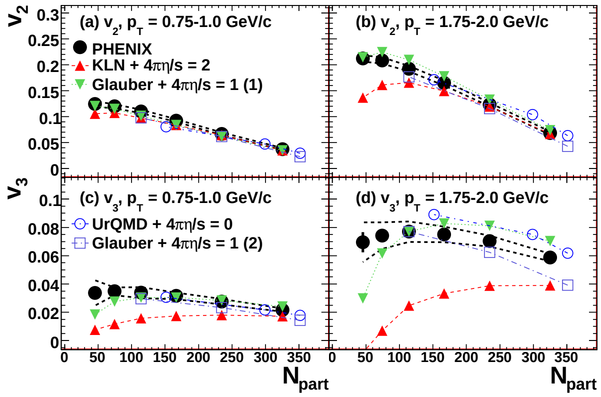

FIG. 3: (color online) Comparison of $v_n\{\Psi_n\}$ vs. $N_{\rm part}$ measurements and theoretical predictions (see text): "MC-KLN + $4\pi\frac{\eta}{s} = 2$" and "Glauber + $4\pi\frac{\eta}{s} = 1$ (1)" [16]; "Glauber + $4\pi\frac{\eta}{s} = 1$ (2)" [17]; "UrQMD" [26];. The dashed lines (black) around the data points indicate the size of the systematic uncertainty.

calculations which employ Glauber initial condition fluctuations and $4\pi\frac{\eta}{s} = 1$ show relatively good agreement with the $v_{2,3}\{\Psi_{2,3}\}$ data. The exact statistical significance of these constraints should be determined through a global fit procedure, after quantitative accounting of the breakdown of hydrodynamics in peripheral collisions, as well as the systematics associated with the averaging of eccentricity fluctuations within these models are fully understood. From our data it is already clear that the higher order moments $v_n\{\Psi_n\}$ for $n \geq 3$ provide an important avenue for constraining different physical properties of the QGP.

In summary, we have presented participant event plane Ψ_n correlations and differential measurements of $v_n\{\Psi_n\}$ for $n = 2, 3, 4$ for charged hadrons using the generalized event plane method. The higher order harmonic moments $v_3\{\Psi_3\}$ and $v_4\{\Psi_4\}$, as well as strong correlations between the higher order event planes across a large rapidity gap of $\Delta\eta' \gtrsim 7$,

provide evidence that the initial state has transverse geometry fluctuations of the generalized eccentricities which are then propagated in the hydrodynamic evolution of the plasma afterwards. This evidence, includes (1) a lack of correlation between the measured event planes of order $n = 2$ and 3 as predicted by Glauber modeling, assuming correlations of the event planes with the generalized eccentricity, (2) proper description of the shapes of the p_T dependence in the low p_T region by hydrodynamic calculations, and (3) agreement with several different initial state + hydrodynamic models across centralities for order $v_n\{\Psi_n\}$. The combined results for $v_{2,3}\{\Psi_{2,3}\}$, in concert with initial hydrodynamic model calculations now suggest that the large (100%) uncertainty previously associated with the extraction of $4\pi\frac{\eta}{s}$ can be significantly reduced. Within the models considered, $4\pi\frac{\eta}{s} \sim 1$ is favored, which is close to the conjectured lower bound for the specific viscosity.

We thank the staff of the Collider-Accelerator and Physics Departments at BNL for their vital contributions. We acknowledge support from the Office of Nuclear Physics in DOE Office of Science and NSF (U.S.A.), MEXT and JSPS (Japan), CNPq and FAPESP (Brazil), NSFC (China), MSMT (Czech Republic), IN2P3/CNRS and CEA (France), BMBF, DAAD, and AvH (Germany), OTKA (Hungary), DAE and DST (India), ISF (Israel), NRF (Korea), MES, RAS, and FAAE (Russia), VR and KAW (Sweden), U.S. CRDF for the FSU, US-Hungary Fulbright, and US-Israel BSF.

* Deceased
† PHENIX Spokesperson: jacak@skipper.physics.sunysb.edu

[1] J.-Y. Ollitrault, Phys. Rev. D **46**, 229 (1992).
[2] U. Heinz and P. Kolb, Nucl. Phys. **A702**, 269 (2002).
[3] E. Shuryak, Prog. Part. Nucl. Phys. **62**, 48 (2009).
[4] K. Adcox et al., Nucl. Phys. **A757**, 184 (2005).
[5] J. Adams et al., Nucl. Phys. **A757**, 102 (2005).
[6] P. Romatschke and U. Romatschke, Phys. Rev. Lett. **99**, 172301 (2007).
[7] H. Song et al. (2010), 1011.2783.
[8] P. Kovtun, D. Son, and A. Starinets, Phys. Rev. Lett. **94**, 111601 (2005).
[9] R. A. Lacey et al., Phys. Rev. C **82**, 034910 (2010).
[10] M. Miller et al., Ann. Rev. Nucl. Part. Sci. **57**, 205 (2007).
[11] B. Alver et al., Phys. Rev. Lett. **98**, 242302 (2007).
[12] T. Lappi and R. Venugopalan, Phys. Rev. C **74**, 054905 (2006).
[13] H.-J. Drescher and Y. Nara, Phys. Rev. C **76**, 041903 (2007).
[14] B. Alver and G. Roland, Phys. Rev. C **C81**, 054905 (2010).
[15] R. A. Lacey, R. Wei, N. N. Ajitanand, and A. Taranenko, Phys. Rev. C **83**, 044902 (2011).
[16] B. Alver et al., Phys. Rev. C **82**, 034913 (2010).
[17] B. Schenke, S. Jeon, and C. Gale, Phys. Rev. Lett. **106**, 042301 (2011).
[18] K. Adcox et al., Nucl. Instrum. Meth. **A499**, 469 (2003).
[19] A. Adare et al., Phys. Rev. Lett. **105**, 062301 (2010).
[20] M. Allen et al., Nucl. Instrum. Meth. **A499**, 549 (2003).
[21] E. Richardson et al., Nucl.Instr. Meth. **A636**, 99 (2011).
[22] K. Adcox et al., Nucl. Instrum. Meth. **A499**, 489 (2003).
[23] S. Afanasiev et al., Phys. Rev. C **80**, 024909 (2009).
[24] J. L. Nagle and M. P. McCumber, Phys. Rev. C **83**, 044908 (2011).
[25] R. A. Lacey et al., arXiv:1011.3535 [nucl-ex] (1021).
[26] H. Petersen et al., Phys. Rev. C **82**, 041901 (2010).
[27] S. A. Bass et al., Prog. Part. Nucl. Phys. **41**, 255 (1998).
[28] M. Bleicher et al., J. Phys. **G25**, 1859 (1999).